



Cytotoxicity activity model of hydroxamic acid analogues as histone deacetylase (hdac) inhibitors based on docking and pharmacophore 3D QSAR approach

Md. Afroz Alam*, N. Christhu Veni, Ligi George, Anurupa Devi. Y, Thalitha Jane. D

Department of Bioinformatics, Karunya University, Karunya Nagar, Coimbatore, 641114, Tamil Nadu, India

ARTICLE HISTORY

Received: 17.11.2011

Accepted: 13.12.2012

Available online: 10.05.2012

Keywords:

Histone deacetylases, Hydroxamic acid, Docking, Pharmacophore, QSAR

*Corresponding author:

Email : maarkzin@gmail.com

Tel : +91-9500724409

ABSTRACT

Histone deacetylases (HDACs) enzyme is a promising target for the development of anticancer drugs. The enzyme-bound conformation of Trichostatin A (TSA) in complex with the protein Histone deacetylase was used for a detailed study of the binding site of the protein. Hydroxamic acid analogues, the class to which TSA belongs were used for docking and the docked ligands obtained after refinement of docking result were used to build the pharmacophore model. The best 3D QSAR model was obtained by plotting the Experimental IC_{50} (Expt. IC_{50}) and the Predicted IC_{50} (Pred. IC_{50}) and calculating the regression coefficient (R^2) value for the hypotheses. The value of the regression coefficient for both the training sets ($R^2 = 0.7098$) and the test set ($R^2 = 0.9592$) were satisfactory. Graphical interpretation and the 3D QSAR model built revealed important structural features of the inhibitors related to the active site of HDACs. The results can therefore be exploited for further design and virtual screening for some novel HDAC inhibitors.

INTRODUCTION

Cancer is the leading cause of death in economically developed countries and the second leading cause of death in developing countries. It was reported that about 12.7 million cancer cases and 7.6 million cancer deaths are estimated to have occurred in 2008 worldwide with 56% of the cases and 64% of the deaths in the economically developing world (1). Thus more emphasis has to be laid in developing the anti cancerous agents that could effectively inhibit the uncontrolled growth of the cells. A search is being made for an ideal anticancer agent who is toxic to malignant cells with minimum toxicity towards normal cells. Currently, there are only a limited number of such agents available for clinical use; thus, the development of novel cancer-selective drugs is an important and challenging task (2). The elucidation of the mechanisms of transcriptional activation and repression in eukaryotic cells has shed light on the important role of acetylation-deacetylation of histones mediated by histone acetyltransferases (HATs) and histone deacetylases (HDACs), respectively. It has been revealed that imbalance in reversible regulation of histone acetylation by histone acetyltransferase (HAT) and deacetylase (HDAC) leads to an aberrant behavior of the cells in morphology, cell cycle, differentiation, and carcinogenesis (3). Thus Histone deacetylases and histone acetyltransferases are considered to play an important role in cell cycle control by acting as a transcriptional coactivator or a transcriptional corepressor (4).

HAT-mediated hyperacetylation of positively charged lysine residues in the N-terminal tails of core histones loosens the histone DNA binding and activates a gene transcription. In contrast, HDAC-catalyzed deacetylation of 3N acetyl group of lysine residues leads to the tight histoneDNA binding, which restricts the access transcription factors. Perturbation of this balance is often observed in human cancers and inhibition of HDACs has emerged as a novel therapeutic strategy against cancer (5). The HDACs catalytic domain consists of a narrow, tube-like pocket spanning the length equivalent to four- to six carbon straight chains. A Zn^{2+} ion is positioned near the bottom of this enzyme pocket. Accordingly, the structure of the lead compound TSA, represented as hydroxamic acid class of HDACs inhibitors, might be divided into three molecular fragments, each of which interacts with a discrete region of the enzyme pocket. These fragments include a zinc binding group (ZBG), a cap group, and a linker connecting the ZBG and the cap at a proper distance. This three-fragment concept has proven successful in developing structural analogues of Trichostatin (TSA) as potent HDACs inhibitors.

Even though a structure-based approach is made possible by knowledge of the structure of the target from crystallography, a ligand-based approach like 3D pharmacophores may provide an alternative and complementary tool for drug design. Some structurally distinct compounds targeting HDACs enzyme have been reported, and with few exceptions, they can be divided into

several structural classes, including small molecular hydroxamic acids, carboxylates, benzamides, electrophilic ketones, and cyclic peptides (6). Among them, hydroxamic acids were the first and largest class of HDACs inhibitors identified, typified by Trichostatin A (TSA) and suberoylanilide hydroxamic acid (SAHA), which are still rapidly growing. The X-ray crystal structure of HDLP (histone deacetylase-like protein), a bacterial HDAC homologue, complexed with the lead compound TSA, has been resolved and revealed a distinctive mode of proteinligand interactions (7). The structure of the lead compound TSA, represented as hydroxamic acid class of HDACs inhibitors, might be divided into three molecular fragments, each of which interacts with a discrete region of the enzyme pocket (8). These fragments include a zinc binding group (ZBG), cap group, and a linker connecting the ZBG and the cap at a proper distance. The crystal structures of human HDAC8 complexes with hydroxamates, reported recently (9), also supported such a binding mechanism of HDACs. This three-fragment concept has proven successful in developing structural analogues of TSA as potent HDACs inhibitors (10). Until now, only a few 3D-QSAR studies for HDACs inhibitors have been reported and most of these models did not incorporate the structural information of the receptor and investigate the local physicochemical properties of three molecular fragments of inhibitors to their respective interaction region.

MATERIALS AND METHODS

Preparation of compound library

Some structurally distinct compounds targeting HDACs enzyme have been reported (6). For this a study a group of 34

hydroxamic acid analogues, the first and largest class of HDAC inhibitors were taken from literature studies (4). All of the molecular structures and activity data used for 3D-QSAR study are represented in Tables 1 and 2, in which inhibitory activity for each compound has been expressed as the normalized IC₅₀ (μM). A diverse collection of 12 molecules chosen at random was used as the test set from the data set, while the remaining 22 compounds were treated as a training set.

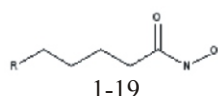
Ligand preparation

Trichostatin has been found to be an effective inhibitor of the protein Histone deacetylase. Thus, a group of hydroxamic acid analogues, to which Trichostatin belongs to, were taken from literature and built from the scaffolds by different ring modification and substitution of functional group as mentioned in Tables 1 - 2. ISIS DRAW 2.3 software was used to sketch the structures and was converted to their 3D representation by using Chems sketch 3D viewer of ACDLABS 8.0. LigPrep were used for final preparation of the ligands from libraries. LigPrep is a utility of Schrodinger software suit that combines tools for generating 3D structures from 1D (Smiles) and 2D (SDF) representation, searching for tautomers and steric isomers and also performing a geometry minimization of ligands. The ligands were minimized by means of molecular mechanics force field (MMFFs) with default setting.

Computational details

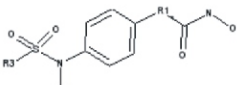
Preparation of the receptor and ligands are done using the Schrodinger Inc, 2008. All the work is done primarily using the Glide and Phase modules. Glide (Grid based ligand docking with energetic) searches for favorable interactions between one or

Table1 represents the Structures and normalized inhibitory activity (IC₅₀) of compounds investigated hydroxamate-based HDACs inhibitors containing aliphatic chain linker

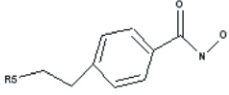


Analogue	R	Expt. IC ₅₀ (μM)	Analogue	R	Expt. IC ₅₀ (μM)	Analogue	R	Expt. IC ₅₀ (μM)
1		0.10	8		0.04	15		0.01
2		0.07	9		0.15	16		0.01
3		0.13	10		0.1	17		0.01
4		0.45	11		0.02	18		0.03
5		0.04	12		0.05	19		0.04
6		0.15	13		0.05			
7		0.1	14		0.01			


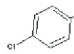
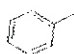
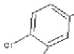

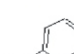

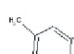
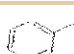



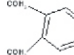


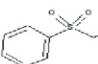
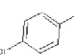

Table 2: Structures and normalized inhibitory activity (IC_{50}) of compounds investigated hydroxamate-based HDACs inhibitors containing aromatic linker.



20 - 32



33 - 34

Analogue	R1	R2	R3	Expt. IC_{50} (μ M)	Analogue	R1	R2	R3	Expt. IC_{50} (μ M)
20	-	H		0.90	27	CH=CH	H		0.08
21	CH ₂	H		1.00	28	CH=CH	H		0.10
22	CH ₂	H		0.10	29	CH=CH	H		0.60
23	(CH ₂) ₂	H		1.00	30	CH=CH	H		0.10
24	CH=CH	H		0.20	31	CH=CH	H		0.06
25		H		2.00	32	CH=CH	H		0.09
26		H		17.00	33		2.00		
27	CH=CH	H		0.08	34		1.00		

more typically small ligand molecules and a typically large receptor molecule, usually a protein. The ligand poses that Glide generates passes through a series of hierarchical filters that evaluates the ligands interaction with the protein. Phase is a high performance program for ligand based drug design. It is a complete package of pharmacophore modeling tools and is a powerful tool for hit generation and lead hoping.

Receptor preparation

The X ray structure of the complex between Trichostatin A and the Histone deacetylase protein (PDB ID: 1C3R) has been used as the initial structure in the preparation of the trichostatin binding site. After manual inspection and cleaning of the structure a complex was retained consisting of the protein's A chain, the ligand bound to the protein, the Zinc heteroatom and all the interacting A chain water molecules, because Zn interacts with water molecules which in turn interact with the active site residues. Hydrogen was added automatically to the model via the Maestro interface, leaving no lone pair and using an explicit all-atom model. All the water molecules were removed from the complex. The multi step Schrodinger's Protein preparation tool has been used for final preparation of the protein. By this use, all the side chains that are not close to the binding site and those that do not participate in salt bridges are neutralized. This step is then followed by restrained minimization of the co-crystallized complex, which reorients the side chain hydroxyl groups and alleviates the potential steric clashes. The complex structure was energy minimized using OPLS_2005 force field and the conjugate gradient algorithm, keeping all atoms except

hydrogen's fixed. The minimization is stopped either after 1000 steps or after the energy gradient converged below 0.01 kcal/mol. The energy minimized structure was further used for the docking of the hydroxamic acid analogues.

Ligand docking

All the ligands were docked to the receptor using Glide version 4.0. After ensuring that the protein and the ligands are in correct form for docking, the receptor grid files were generated using the grid-receptor generation program, using van der Waals scaling of the receptor at 0.4. The default size was used for the bounding and enclosing boxes was generated at the centroid of the Trichostatin binding site by specifying the residue numbers of the bound Trichostatin A ligand. Similar work has been done in the case of podophyllotoxin analogues acting against tubulin protein (11). The active site residues that were specified in our work include His 131(A), His 132(A), Asp 173(A), Asp 166(A), Asp 168(A), Phe 141(A), Zn 501(A), Tyr 297(A), His 170(A), Pro 22(A), Leu 265(A), Phe 200(B), Glu 195(B), Asn 20(A). The ligands were docked initially using the "standard precision" methods and further refined using "extra precision" Glide algorithm. For the ligand docking stage, van der Waals scaling of the ligand was set at 0.5. Of the 50,000 poses that were sampled, 400 were taken through minimization (conjugate gradient). Finally, all the ligands with their XPG Score were obtained and these ligand structures were used for further work.

3D QSAR Study

In order to investigate the quantitative relationships between

the activities of hydroxamic acid analogues and to derive a predictive model that will be useful in future, the activity values were analyzed using a 3D QSAR strategy. Discovering three dimensional pharmacophores that can explain the activity of a series of a ligands is one of the most significant contributions of computational chemistry to drug discovery, and Phase is one of the most recently developed pharmacophore modeling tools (12). Phase has a hypotheses generating step based on a grid based 3D QSAR method in which the grid positions of the atoms in the molecules superimposed on the hypotheses are correlated with their activities using a partial-least-squares (PLS) fitting. The main stages of phase methods are summarized in Figure 1.

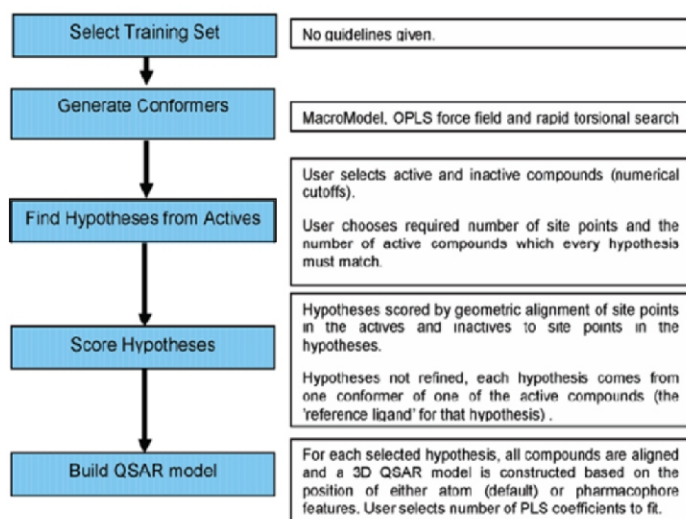


Figure 1: Summary description of Phase Methodology [13]

As we used Phase methodology to create a reasonable 3D-pharmacophore model with the aim of further rationalizing the observed SAR, we selected a set of 22 molecules as the training set and used these to train about 12 molecules in the test set. For each hydroxamic acid analogue, a group of suitable pharmacophore sites (features) were assigned from which to derive a set of suitable pharmacophore. Finally, by analyzing the ability of all the possible pharmacophore site combinations to classify active and inactive compounds correctly, we finally identified a 5 feature (2 H-bond acceptor, 2 H-bond donor, 1 aromatic ring) model as the best pharmacophore features of the training set as well as test set compounds. The pharmacophore perception inside the receptor active site gives an insight to the selection of these features as pharmacophore.

RESULTS AND DISCUSSION

The original crystal structure of Trichostatin-Histone deacetylase complex (PDB ID: 1C3R) was used to validate the Glide docking protocol. This was done by moving the co-crystallized trichostatin outside of the active site and the docking it back to the active site. All analogue configurations after docking were taken into consideration after making a note of their docking Score which varies in the range of -5.57 to -10.37 and their ΔG score which varies in the range of -0.86 to 0.02 (Table 3). The fitness was calculated for each configuration in comparison with the co-crystallized trichostatin and the fitness range for the ligands was found to be from 0.74 to 3. After a careful analysis of the binding of the other ligands in comparison with the internal ligand bound as shown in figure 3, it is understood that the binding positions and orientations within the binding site are similar to the

crystal structure. In the figure, we can observe that all the ligands were well fitted in the defined binding pocket.

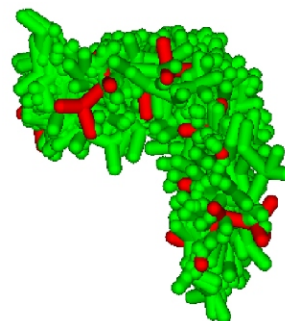


Figure 2: Superimposition of all the docked configurations of hydroxamic acid on the co-crystallized structure of trichostatin. ΔG_{score} which varies in the range of -0.86 to 0.02 (Table 3)

The docking results as illustrated in figure 2 show that all the docked ligands agree well with the Trichostatin's crystal structure.

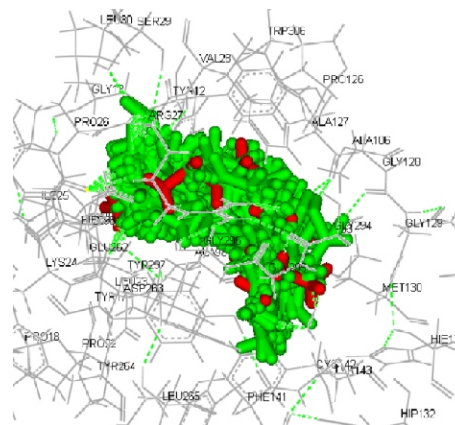


Figure 3: Hydroxamic acid analogues (green colour) along with the co-crystallized Trichostatin (red) within the binding site of Trichostatin showing that the Hydroxamic acid analogues and Trichostatin have similar active site residues.

Pharmacophore model generation

TSA contains 22 features that are close enough for complementary functionalities in the enzyme to participate in binding interactions (4). If all of these features were included in a single pharmacophore model, the model would be too restrictive to fit structurally diverse molecules. For each hydroxamic acid analogue, a group of suitable pharmacophore features were assigned from which to derive a set of suitable pharmacophores and an activity of 0.08 was specified as the threshold for defining an 'active' compound. Thus, after defining the variant list and the minimum number of ligands they should match, a few hypotheses were obtained as shown in Table 4. For each hypothesis generated, the active molecules were scored and their 3D QSAR models were built. The predicted activities for each ligand with respect to each hypothesis were obtained and one hypothesis has been taken for our study in which then compounds have been divided into training and test set as shown in Table 5 and Table 6 respectively and along with their R^2 values have been shown in figure 4 and figure 5. Finally, Experimental activity versus Predicted Activity values is graphically depicted for both the training set $R^2 = 0.7098$ and for test set $R^2 = 0.9592$ which is

Table 3: List of the ligands, their structure and their respective Docking score and their $\Delta G_{\text{score}} = E_{\text{el}}$ Lowest.

S. No	Analogue	Docking Score	ΔG_{score}	S. No	Analogue	Docking Score	ΔG_{score}
1		-10.37	0.00	18		-7.66	-0.13
2		-9.51	-0.86	19		-7.43	-0.23
3		-9.18	-0.33	20		-7.04	-0.39
4		-8.58	-0.60	21		-7.02	-0.02
5		-8.58	-0.00	22		-6.90	-0.12
6		-8.45	-0.13	23		-6.79	-0.11
7		-8.29	-0.16	24		-6.42	-0.37
8		-8.18	-0.11	25		-6.41	-0.01
9		-8.04	-0.14	26		-6.42	0.01
10		-7.97	-0.07	27		-6.40	-0.02
11		-7.95	-0.02	28		-6.37	-0.05
12		-7.91	-0.04	29		-6.01	-0.36
13		-7.85	-0.06	30		-5.99	-0.02
14		-7.85	0.00	31		-5.89	-0.10
15		-7.84	-0.01	32		-5.74	-0.15
16		-7.79	-0.05	33		-5.57	-0.17
17		-7.79	0.00	34		-5.59	0.02

acceptable and robust model for QSAR study. Obtaining the optimal value of R^2 (1.0) would require that the predicted values correlate with the actual values with a slope of 1.0 and zero offset (13). Similar study have been studied in which the highest test set correlation coefficient from the ten hypotheses evaluated with each of the parameter sets is presented for each system and the R^2 values, which can be interpreted as the fraction of the variance in the experimental test set activities which is explained by the

model (13). The regression coefficient (R^2) of the 3D QSAR model is calculated and the value obtained for the hypotheses AADDR.16 indicated a significant and stable model as shown in Figure 4 and Figure 5. Therefore, an important recommendation from this study is to directly test the predictivity of as many hypotheses as possible to find the most successful one, rather than relying on the scoring of the hypotheses alone.

Table 4: List of the hypotheses generated and their respective regression coefficients (R^2) values, each for the training set compounds and the test set compounds

HYPOTHESES	$R^2_{\text{TRAIN. SET}}$	$R^2_{\text{TEST SET}}$	HYPOTHESES	$R^2_{\text{TRAIN. SET}}$	$R^2_{\text{TEST SET}}$
AAADR.44	0.1221	0.1165	AAADR.48	0.3306	0.2148
AAANR.1	0.3995	0.6198	AARRN.12	0.6005	0.0258
AADDR.16	0.7098	0.9592	AADDR.20	0.5264	0.3328
AANRR.3	0.4419	0.7528	AANRR.10	0.2215	0.4366
AANRR.4	0.5269	0.8572	AAADR.17	0.6643	0.1433

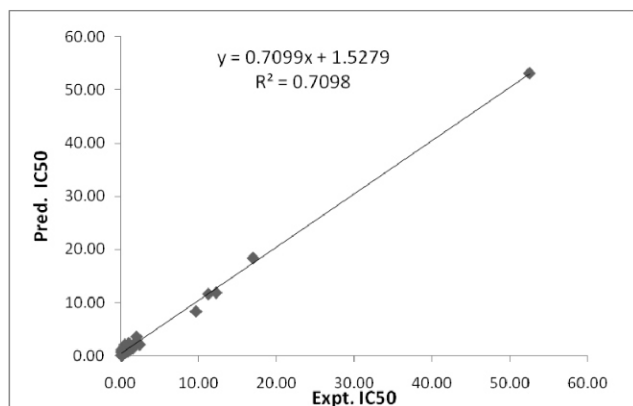
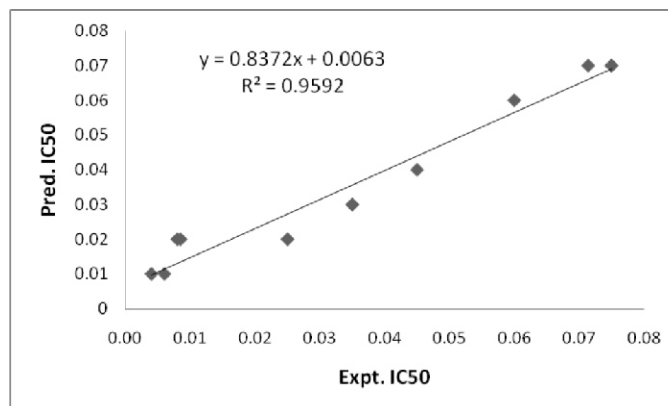
Table 5: List of the experimental and predicted activity values of compounds in the training set along with the individual fitness value with respect to the best Phase hypotheses AADDR.16 generated.

Analogue	Expt. $IC_{50}(\mu M)$	Pred. $IC_{50}(\mu M)$	Fitness	Analogue	Expt. $IC_{50}(\mu M)$	Pred. $IC_{50}(\mu M)$	Fitness
1	0.10	0.69	1.72	12	0.50	2.10	1.71
2	2.40	2.11	1.71	13	0.60	0.58	1.58
3	17.00	18.40	1.57	14	0.10	1.09	1.47
4	1.00	1.55	1.74	15	2.00	3.59	1.68
5	0.45	1.71	1.70	16	12.25	11.87	3.00
6	0.10	0.09	1.61	17	0.20	0.18	1.64
7	0.10	0.74	1.69	18	1.50	1.40	1.59
8	0.90	0.78	1.32	19	52.56	53.21	2.09
9	1.00	2.34	1.58	20	0.10	0.09	1.64
10	0.09	0.07	1.83	21	9.65	8.35	2.90
11	2.00	2.73	1.57	22	11.25	11.65	2.25

Table 6: List of the experimental and predicted activity values of compounds in the test set along with their individual fitness value with respect to the best Phase hypotheses AADDR.16 generated.

Analogue	Expt. $IC_{50}(\mu M)$	Pred. $IC_{50}(\mu M)$	Fitness	Analogue	Expt. $IC_{50}(\mu M)$	Pred. $IC_{50}(\mu M)$	Fitness
23	0.04	0.03	1.68	29	0.01	0.02	1.69
24	0.03	0.02	1.69	30	0.06	0.06	1.62
25	0.05	0.04	1.72	31	0.07	0.07	0.74
26	0.01	0.01	1.70	32	0.04	0.03	1.64
27	0.01	0.02	1.55	33	0.00	0.01	1.34
28	0.08	0.07	1.95	34	0.08	0.07	1.41

Graphical representation of the activity values and their correlation relationship between predicted and experimental activities as per Pharmacophore generation of the training set compounds as well as test set compounds.

**Figure 4:** Predicted versus actual activity values for the training set of the Phase model with the highest R^2 value. The data points would need to be on the R^2 line for a R^2 value of 1.0.**Figure 5:** Predicted versus actual activity values for the test set of the Phase model with the highest R^2 value.

By analyzing the ability of all the possible pharmacophore site combinations to classify active and inactive compounds correctly, a 5 feature model was identified as the best pharmacophoric descriptor and the fifth analogue had the best fitness as shown in figure 6. These features include two aromatic rings, two hydrogen bonds acceptor and a nitrogen atom. Once all the ligands were overlaid with our best Phase hypotheses, an atom based 3D QSAR analysis was derived on the basis of standard Phase parameters. This 3D QSAR model is depicted and shown in the following figures.

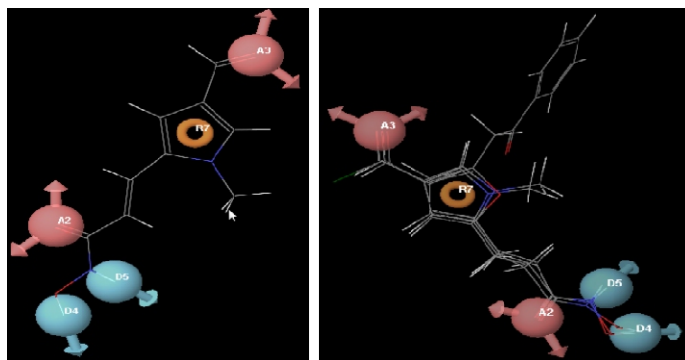


Figure 6: Best Phase hypotheses overlaid with the other ligands having good fitness and superimposed on the most active hydroxamic acid analogue ligand. Fitness ranges of all individual analogue of trichostatin with trichostatin = 0.74 3 (Table 5 and 6)

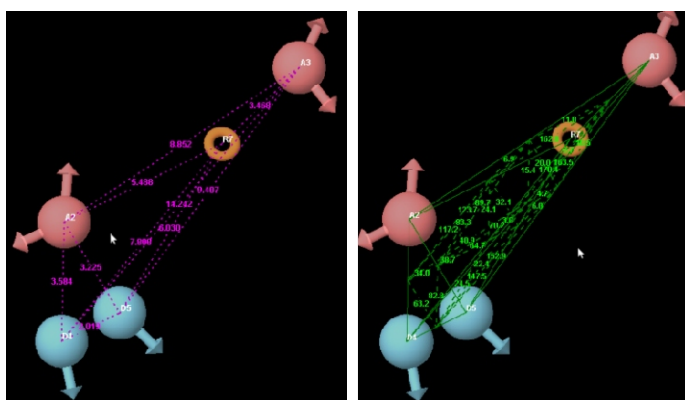


Figure 7: Intersite distances and angles between the pharmacophore features in the best hypotheses AADDR.16

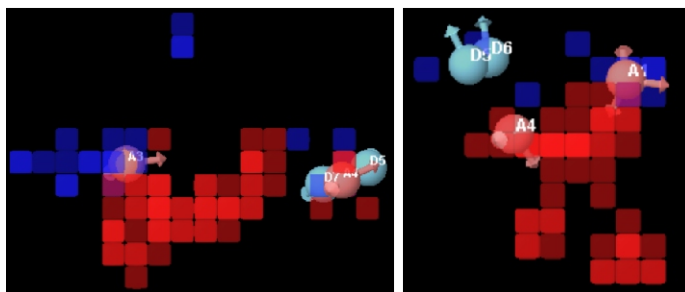


Figure 8: Figure showing high and low activity regions in the respective pharmacophore features and QSAR visualized by different color pattern, orange: aromatic ring; pink: hydrogen bond acceptor; red: a nitrogen atom.

Most of the ligand molecules were found to have good fitness for the hypotheses with the highest R^2 value generated (AADDR.16). All these ligand molecules have been overlaid

along with the best fitness ligand molecule as shown in figure 6. Thus, it is seen that the functional part of each ligand coincides with the respective pharmacophore feature of the hypotheses generated. From the best Phase hypotheses, the functional features of the pharmacophore were identified to be two aromatic rings, two hydrogen bond acceptors and a nitrogen atom. This hypothesis had a regression coefficient (R^2) value as 0.7098 for the training set and 0.9592 for the test set, after the Predicted and Experimental IC_{50} values and their correlation were graphical depicted. The regions required for high activity have also been found as shown in figure 8. The blue cubes refer to ligand regions in which the specific feature is important for high activity, whereas the red cubes suggest that the activity of the same ligand feature substitution is less. The angles and the interstice distances between the various pharmacophore features were measured and studied on as shown in figure 7. Reasonably, the predictivity shown by our model could be helpful in designing new related derivatives while the 3D Pharmacophore model can also be used for the virtual screening of large databases with the aim of identifying new Histone deacetylase inhibitors.

CONCLUSION

HDAC-catalyzed deacetylation of 3N acetyl group of lysine residues leads to the tight histoneDNA binding, which restricts the access transcription factors. Herein, we have shown a pharmacophore based 3D QSAR study of the hydroxamic acid analogues that are aimed at inhibiting Histone deacetylase protein. Most of the screened molecules resulted to be more effective in terms of their XPG Score, the highest score being -10.37. From the various hypotheses obtained from Phase methodology to develop a statistically robust 3D pharmacophore model, the best hypotheses was obtained calculating the regression coefficient (R^2) for each of them taking into consideration their Experimental and Predicted IC_{50} values and also taking into account their fitness. The R^2 value for both the training and test sets were significant for the hypotheses AADDR.16. This pharmacophore model was identified to have 5 pharmacophore features namely, two hydrogen bond acceptors, two hydrogen bond donor, and a aromatic ring. Thus, such a pharmacophore model provides insights into the structural and chemical features of the HDAC inhibitors of the hydroxamic acid analogues and can be used as lead compound for further synthesis as well as for screening other similar novel inhibitors of HDAC.

ACKNOWLEDGEMENTS

We are thankful to Dr. Patrik Gomez and Dr. Janet Vaniella for providing a very nice working atmosphere and resources.

REFERENCES

1. Jemal A, Bray F, Center MM, Ferlay MJ, Ward E, Forman D. Global Cancer Statistics. *Cancer J. Clin.* 2011; (66): 6990.
2. Hidemi R. Autophagic and Apoptotic Effects of HDAC Inhibitors on Cancer Cells. *J Biomed. Biotech.* 2011; 9.
3. Kim DH, Kim M, Kwon Ho J. Histone deacetylase in carcinogenesis and its inhibitors as anti-cancer agents. *J. Biochem. Mol. Bio.* 2003; (36): 110-119.
4. Yadong C, Huifang L, Wanquan T, Chengchao Z, Yongjun J, Jianwei Z, Qingsun Y. 3D QSAR studies of HDACs inhibitors using Pharmacophore based alignment. *Eur. Jour of Med Chem.* 2009; (44): 2868-2876.
5. Kouzarido AT, Cress WD, Seto E. Histone deacetylase,

transcriptional control and cancer. *J Cell Physiol.* 2000; (184): 1-16.

6. Jung M. Inhibitors of histone deacetylase as new anti cancer agents. *Curr Med Chem.* 2001; (8): 1505-1511.

7. Finnin ER, Marks PA, Richon BM, Breslow R, Rifkind RA. Histone deacetylase inhibitors as a new cancer drugs. *Curr. Opin. Oncol.* 2002; (13): 477-483.

8. Chen JS, Fallen DV, Spanjaard RA, Kurr C. Pharmacophore based Discovery of ligands for drug transporters. *Cancer Drug Targets* 2003; (3): 219-236.

9. Vannini A, Volpari C, Filocamo G, Casavola EC, Brunnetti M. Crystal structure of a eukaryotic Zinc dependent Histone deacetylase, Human HDAC8 complexes with a hydroxamic acid

inhibitor. *Proc Natl Acad Sci.* 2004; (101): 1564-1569.

10. Jung M, Brosch G, Kolle D, Scherf H, Gerhouser C. Amide analogues of trichostatin A as inhibitors of histone deacetylase. *Mol. Cell.* 1999; (32): 229-244.

11. Alam MA, Pradeep PK. Molecular modelling evaluation of the cytotoxic activity of Podophyllotoxin analogues. *J Comput Aided Mol Des.* 2008; (4): 209-225.

12. Palm K, Vingushin DM, Coombes RC. HDAC inhibitor in cancer treatment. *Anticancer Drugs.* 1998; (13): 1-13.

13. David AE, Thomson ND, David AE, Michael JB. 3D QSAR Methods-Phase and Catalyst compared. *Expert Opin. Drug Discover.* 2007; (1): 103-110.